

# High-frequency over-the-horizon radar and ionospheric backscatter studies in China

Le-Wei Li

Communications and Microwave Division, Department of Electrical Engineering  
National University of Singapore, Singapore

**Abstract.** China is one of the countries that employs high-frequency over-the-horizon radars for both military and civil applications. The first Chinese high-frequency over-the-horizon backscatter radar was developed in the 1970s. This paper briefly introduces the first Chinese over-the-horizon backscatter radar system and reviews ionospheric backscatter and propagation studies in China. The paper discusses the motivation for establishing over-the-horizon radar systems in China, the experimental system, target recognition and detection, and estimation of over-the-horizon radar availability. Observations of aircraft, large-scale traveling ionospheric disturbances, and the effects of a remote nuclear explosion are also presented. Finally, the real-time Chinese ionosonde network and frequency predictions using backscatter ionograms are discussed.

## 1. Introduction

Within the family of modern radars, various systems operating at different frequencies are continuously being developed in order to meet civil and military requirements. High-frequency (HF) sky wave over-the-horizon radar (OTHR) is unique in its capability to detect distant targets below the horizon line such as aircraft, ships, rockets, and nuclear explosions. The propagation of HF or shortwave over very long distances arises from a series of reflections occurring successively between the Earth's surface and the ionosphere, which typically have an average peak altitude of about 300 km. The coverage provided by one hop (i.e., the distance between two adjacent reflection points of radio waves by the Earth's surface) is typically about 1000 km up to 3000 km, although it can be as great as 4000 km.

HF OTHRs have been developed in many countries, including Australia, Canada, China, England, France, Russia and the United States, and employed in various civil and military applications [Headrick and Skolnik, 1974; Croft, 1967, 1972; Rao, 1974, 1975; Anderson and Lees, 1988; Earl and Ward,

1987; Ahearn *et al.*, 1974; Georges, 1980; Barrick *et al.*, 1967, Lipa *et al.*, 1981; Maresca and Georges, 1980]. Basically, two types of OTH radars have been designed, one using a monostatic pulse Doppler system and the other utilizing a bistatic frequency modulation (FM) continuous wave (CW) system.

The earliest Chinese HF OTH backscatter (OTH-B) radar system was a monostatic pulsed system (referred to as the phase I system), built in the 1970s, which is still in operation today. This experimental OTH-B sky wave radar system was a collaboration by the China Research Institute of Radiowave Propagation (CRIRP) and the Nanjing Research Institute of Electronics Technology (NRIET) [Wang and Wu, 1986]. The phase I pulsed system was changed in 1990 to the FM CW system (referred to as the phase II system). In addition, two OTH ground wave backscatter radar systems are currently operated by Wuhan Institute of Mathematics and Physics (WIMP) of Chinese Academy of Science and Harbin University of Technology (HUT) for ocean surface remote sensing and ship detection within 150 km. Although the two radar systems are also part of the Chinese OTH backscatter radar systems, they are not related with ionospheric research and therefore are not discussed in this paper. This paper discusses the motivation for establishing over-the-horizon radar systems in China, the first (phase I) experimental OTH-B radar system, target recogni-

Copyright 1998 by the American Geophysical Union.

Paper number 98RS01606.

0048-6604/98/98RS-01606\$11.00

tion and detection, and estimation of OTHR availability. Observations of aircraft, large-scale traveling ionospheric disturbances (TIDs), and the effects of a remote nuclear explosion and two launched carrier rockets are also presented. Finally, the real-time Chinese ionosonde network and frequency predictions using backscatter ionograms are discussed.

## 2. Motivation of the OTHR Development in China

Like most other countries, the Chinese OTH radars have been developed by a defense organization, in this case the Chinese Defence Science and Technology Organization (CDSTO). Even so, the motivation of the OTHR development in China has included scientific and civil applications as well as military ones.

### 2.1. Scientific Exploration of the Atmosphere

The first major role of the Chinese OTH-B radars is the scientific exploration of the ionosphere to provide efficient services of ionospheric predictions. Normally, ionospheric parameters are measured by means of vertical ionospheric sounders. The China Research Institute of Radiowave Propagation (CRIRP), together with Wuhan University, has established the Chinese Ionosonde Network (CIN), which measures, at specific locations, the ionospheric profile and its diurnal and seasonal variations. However, it is not practical to set up vertical sounders in some areas, such as the ocean, but this can be overcome to some extent by backscatter ionospheric probing using OTHRs.

### 2.2. Military Wide-Area Surveillance

The second role is to monitor aircraft traffic for defense purposes. The region covered by conventional line-of-sight (LOS) radars corresponds to only 10 min flying time for supersonic aircraft and only 30 min for subsonic aeroplanes. OTHR can extend this to 1.5 hours flying time for supersonic aircraft and to over 3 hours for subsonic aeroplanes. OTH radar aircraft detection is transmitted directly to the National Operation Command Center (NOCC) by a data transmission network. The information can also be transmitted to the sector operations command centers upon an individual's request. The extra time gained allows for more flexibility in defense strategies. The area covered by the phase I and phase II

Chinese experimental HF OTHRs is roughly shown in Figure 1. However, this coverage does not include those by the two OTH ground wave backscatter radar systems.

### 2.3. Ocean Civil Services

The third role of the Chinese OTHRs is to provide civil services to various scientific, educational, and industrial institutions. These services, offered by the two OTH ground wave radar systems, include the supply of data on the state of the ocean surface and navigation guidance.

The OTHR provides a means of remote sensing. Analyzing the mean Doppler spectrum of sea echoes gives information on the state of the sea surface. The first-order and higher-order Doppler echoes, for instance, give the wind-wave direction or the wind direction on surface, the surface current, the RMS wave height, the scalar ocean-wave spectrum, and the frequency of the dominant ocean wave. These useful meteorological observations can provide additional data for weather forecasting in certain special situations.

## 3. The First Experimental OTHR System (Phase I)

The aforementioned scientific, civil, and military requirements led to the earliest experimental system of Chinese OTHR systems being developed in the 1970s. It was sponsored by the Chinese Defence Science and Technology Organization (CDSTO), initially for the experimental development of OTHR systems and for studies of ionospheric wave propagation and ionospheric physics. The projects were subcontracted to the Chinese defense industry, mainly involving the China Research Institute of Radiowave Propagation (CRIRP) and the Nanjing Research Institute of Electronics Technology (NRJET).

The first Chinese OTHR system was a monostatic pulse-Doppler radar with separate transmitting and receiving antenna arrays. In systems development, an ionosonde was attached to give ionospheric information used for target location. The basic parameters of the experimental OTH radar (phase I) are shown in Table 1 [Wang and Wu, 1986].

In the OTHR system, flexible changeable waveforms were available to study short-term ionospheric instabilities and fluctuations. A programmable digital waveform generator was used. The choice of pulse width was between 300  $\mu$ s, 1 ms, and 3.5 ms. The



Figure 1. A map showing the coverage of the HF over-the-horizon (OTH) sky wave backscatter radars and the distribution of the Chinese Ionosonde Network (CIN).

linear frequency modulation bandwidth was chosen from 3.4-, 10-, or 30-KHz in 3.5-ms pulse width. The choice of wave form repetition period could be either 60, 100, or 300 Hz. The transmitter was a tuned amplifier, and the receiver was linear, with a large dynamic range. A frequency synthesizer of high spectral purity was used for the local oscillators.

A pulse-Doppler (PD) processing system was adopted to determine the desired target signals, which are generally very weak in comparison with the much stronger noise clutter. The signal processor was a macro-instruction computer, and the logic control was hard-wired. The clock frequency for computation and control was 4 MHz. A fast Fourier transform (FFT) procedure was the core component of the processor, transforming the signals from the time domain to the frequency domain. The computing method for the FFT was a centralized radix-two data process with block floating point. These procedures, in the radar signal processing, enable desired target

signals to be detected within a strong clutter background. In addition, on the OTH radar site, there was a spectral monitor subsystem that selects a quiet frequency automatically with a networked computer. This computer also rapidly changes the frequency of the local oscillators.

Using the signal processor of the experimental radar itself, the spectra of ground clutter were analyzed for many conditions. The measured results showed [Wang and Wu, 1986] that when the Doppler frequency of the ground clutter was shifted by  $\sim 2$  Hz, the power density of the clutter dropped by  $\sim 40$  dB.

With the help of a cooperative target (e.g., a coherent reference transponder), the horizontal antenna pattern from the full-size receiving log-periodic antenna array was measured. To locate the cooperative target in a suitable place, the receiving antenna beam direction was controlled by the computer and rapidly scanned across the cooperative target. The signal levels received in the different antenna beam

Table 1. The Parameters of the First Experimental Over-the-Horizon Radar (Phase I) System

Component	Parameters
Operation frequency	6-22 MHz
Transmission power	$\hat{P}_T = 600$ kW, $\overline{P}_T = 100$ kW
Transmitting antenna	eight elements, vertical polarization, linear polarized antenna fan array; directive gain $G_T = 18$ dBi (at 14.5 MHz); ground screen, 90 m in front of array; stretch cell size, 45×45 cm; horizontal beam width, 15°–30°; constant direction beam; angle at lower 3 dB point of vertical beam, 6°–8°
Receiving antenna	32 elements, vertical polarization, linear polarized antenna array; horizontal beam width, 5° (at 14.5 MHz); directive gain $G_r = 26$ dBi (at 14.5 MHz); control of beam phased array in azimuth; ground screen, 60 m in front of array; stretch cell size 45×45 cm
Frequency Management	spectrum surveillance system and backscatter sounder
Detection energy	100 dBJ (at 14.5 MHz)
Waveform and SCV	linear FM burst and >55 dB
Time	both integration and dwell: ( $T_i$ ) 1–17 s
Work model	for target detection, fullpower and fixed single frequency; for ionospheric research, small power and sweep frequency.

positions were then compared with the signal level in the direction of the cooperative target. The scanning pattern of the receiving antenna was thus obtained. It is an inexpensive method used to measure the full-size receiving antenna pattern in the horizontal plane. The results obtained from the measurements by means of the comparison method were in very good agreement with those predicted by theoretical analysis. The maximum sidelobe level is shown by the measurements to be between  $-22$  and  $-17$  dB down relative to the main lobe.

The cooperative target, referred to as a coherent transponder, was located 1500 km away from the radar site. It was also used to measure the ionospheric propagation losses  $L_p$  and the coefficient of backscatter  $\sigma_0$ , with the output of the coherent transponder kept constant. A great number of sample statistics of  $L_p$  and  $\sigma_0$  were made in the desert areas and in the Qilian Mountain area. When the available pulse width is 100  $\mu$ s, the amplitude of the recorded waveform showed that the amplitude of the backscattered ground clutter is much stronger than the scatter background. The measurement shows that the difference of the pulse peaks is approximately 10 dB. This is mainly the result of land features. For instance, mountain ranges and cities in certain areas were found to be efficient scatterers. The average backscatter coefficients  $\sigma_0$  are about  $-25$  dB in the desert areas and about  $-20$  dB in the Qilian Mountain area.

#### 4. Coefficient of Ground Backscatter: An Empirical Formula

From the backscattered signal record data collected for the hilly land, over 200 samples were used in the analysis and statistics. The following empirical model for the coefficient  $\sigma_0$  of groundwave backscatter was developed, based on the experimental data. Expressed in linear form, the relation is

$$\sigma_0(\alpha) = A \sin^n \alpha, \quad (1)$$

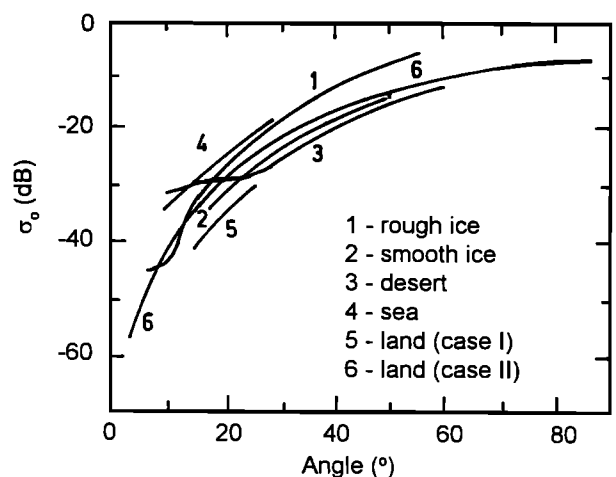


Figure 2. A comparison between the predicted backscatter coefficient (using an empirical model) and the previously documented data.

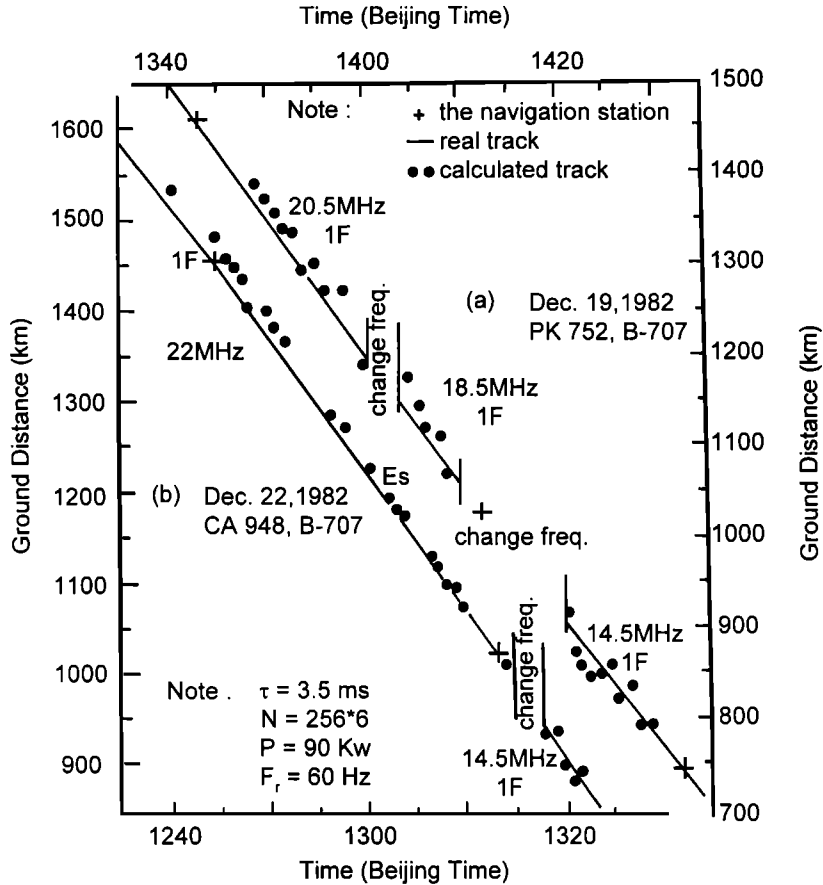


Figure 3. The tracks of civilian aircraft for two periods during December 1982.

where  $A = 0.1342$  and  $n = 4.3085$ , or in decibel form,

$$\sigma_0(\alpha) = -8.77 + 43.085 \log \sin \alpha. \quad (2)$$

For land in the hilly area, we have used this model to compute the backscatter coefficient  $\sigma_0$  (see land (case II) in Figure 2). The predicted coefficient obtained by using the empirical model is also compared in Figure 2 with other published data. As can be seen from the comparison, this developed model gives a close value to measured data found in the literature for various ground environments such as rough ice, smooth ice, desert, sea, and land (case I).

### 5. Observation of Aircrafts and Carrier Rockets

Actual observations of aircraft targets were made by utilizing a newly developed method for track pro-

cessing of the HF OTH-B radar, which include civil transport airplanes and fighter aircraft at distances of about 700 km to 1500 km [Du and Jiao, 1988; Jiao, 1991]. Figure 3 (upper part) shows the record of an actual observation on December 19, 1982, of a civil airplane, flight PK752. In the observation experiment, three operating frequencies, i.e., 14.5, 18.5, and 20.5 MHz, were used. Figure 3 (lower part) demonstrates another record of the actual observation on December 22, 1982 of civil aircraft, flight CA948. In this experiment, two operating frequencies, 14.5 and 22 MHz, were adopted. In Figure 3 the plus signs show the locations along the flight path of the navigation stations. The solid circles denote the tracks of the civil aircrafts. The solid line denotes the track of the civil airplane observed by the ground navigation station. The relative errors of the ground distances obtained by the radar and the navigation stations are shown in Figure 3 at less than

4%. In April 1984, similar detection of aircraft was also made and at that time a B-707 transport aircraft was observed. Two frequencies of 10.5 MHz and 11.5 MHz were used and the parameters shown in Figure 3 were  $\tau = 3.5$  ms,  $N = 256 \times 4$ ,  $P = 70$  kW, and  $F_r = 60$  Hz. Details of those observations are given by *Wang and Wu* [1986].

The vertical launchings of two carrier rockets, DF-2 and DF-5, in November 1989 were observed by means of the OTHR sweep-frequency system [*Jiao and Si*, 1991]. An artificial ionospheric hole was analyzed by using the ray tracing technique. It was found that 79 min after the DF-5 was launched, the disturbance waves reached a range of 350 km and the critical frequency ( $f_0$ ) in such a hole decreased 2.6 MHz relative to the critical frequency in the background ionosphere of 12.4 MHz, while the dimension of the ionospheric hole grew to 573 km. The existence of the ionospheric hole due to the rocket launching lasted for 132 min.

## 6. Real-Time Chinese Ionosonde Network (CIN)

The ionosphere is the medium necessary for the operation of HF OTHR. The accuracy of locating targets or distant environments using OTHR is affected directly by the variations of ionosphere. Therefore it becomes quite necessary (1) to provide real-time access to the ionospheric parameter data from scientific and educational institutions in China; (2) to provide the accumulated data of the ionosphere above mainland China and the related special ionospheric models at various zones; and (3) to provide ionospheric predictions over China to CCIR and other similar organizations in Asia-Pacific areas.

Although effective means have been developed to extract the ground distances of targets from backscatter ionograms without knowing ionospheric parameters, these methods still rely upon the system requirement. Therefore it is still necessary to have a separate real-time ionospheric probing network. From this network, ionospheric parameters can be used directly to assist the OTHR system and to verify data from the OTH radar systems. Analyzing a great quantity of experimental data, scientists and research engineers can derive real-time ionospheric prediction models.

For the aforementioned reasons, in China many ionospheric vertical probing stations have been es-

tablished, and these are known as the real-time Chinese Ionosonde Network (CIN) [*Ma and Jiao*, 1996], consisting of 13 existing ionospheric sounding stations: Changchun, Chongqing, Beijing, Great Wall, Guangzhou, Haikou, Lanzhou, Manzhouli, Qingdao, Sheshan, Urumqi, Wuchang, Xinxiang, and Zhongshan. Most of these stations belong to the China Research Institute of Radiowave Propagation. The remainder are operated by the Wuhan Institute of Mathematics and Physics, Chinese Academy of Science. Fig 1 shows the location of the ionospheric vertical sounders. The locations of these ionosondes are taken from *Ma and Jiao* [1996]. At these ionospheric vertical sounding stations, the majority of the instruments were produced at the China Research Institute of Radiowave Propagation, and the remainder were imported from the United States.

## 7. Target Location

The location of ground targets detected by OTHR is quite important. In China, three specific software packages for HF OTHR target location and detection have been developed for determining the ground distance between the receiver and the targets. The main concepts of the models are (1) the ray equation method, (2) the semiempirical method, and (3) the relative location method.

### 7.1. Ray Equation Method

The idea behind this method was taken from *Croft and Hoogasian* [1968] and *Rao* [1975]. On the basis of Croft and Hoogasian's quasi-parabolic P-D equations of group path (P) and ground range (D), the derivative of group time delay with frequency was found, and the minimum group time delay and corresponding frequency were then calculated. By use of the measured data of minimum group time delays on backscatter ionograms and the real-time ionospheric parameters obtained from the ionospheric vertical sounding stations, the real-time position of targets (or environments) was then obtained. The method implemented is now rarely used in actual OTHR operations due to the requirement for real-time ionospheric parameters at the reflection point.

### 7.2. Semiempirical Method

The quasi-empirical method was first developed by *Jiao and Zhu* [1985] and then improved by *Jiao and Du* [1987] and *Du and Jiao* [1988].

To establish the relationship between the minimum group delay and its corresponding ground distance, two well-known formulae were given by *Croft and Hoogasian* [1968]. However, the ionospheric profile must be known before the relations can be actually used. To overcome this, *Jiao and Zhu* [1985] and *Wieder* [1955] worked out a different formula. On the basis of the geometrical relation, an intermediate relation was obtained [*Jiao and Zhu*, 1985; *Wieder*, 1955] as a function of elevation angle, reflection virtual height, the minimum group delay, and the operating frequency. To minimize the error, a semi-empirical factor was introduced [*Jiao and Zhu*, 1985]. Then, a modified equation satisfied by the vertical incident frequency, oblique incident frequency, group path, and reflection virtual height was derived. Such a semiempirical constant (taken as  $4.7 \times 10^{-5} \text{ km}^{-1}$ ) was determined from a large number of experimental records. One then takes the derivatives of both the aforementioned equations and the group time delay given by *Croft and Hoogasian* [1968]. Substituting the vertical incident frequency from one derivative formula into the other derivative formula, they obtained a general equation for the minimum group path, its derivative, virtual height, corresponding operating frequency, and the semiempirical constant. Using actual measurements, the minimum group time delay, its derivative, and corresponding operating frequency can be read from the backscatter ionograms. Therefore the virtual height of reflection may be solved from the nonlinear equation. Furthermore, the ground distance and other quantities can be obtained from the derived virtual height of reflection.

However, the derivative of group path is quite difficult to determine accurately from the ionograms because of the sudden changes at different points along the group path curve. *Jiao and Du* [1987] and *Jiao and Du* [1988] modified the previous method and improved the accuracy of experimentally determining the group path derivative. By assuming that the equations satisfied by both the minimum and arbitrary time delays are parabolic (e.g.,  $P'_{\min} = C_0 + C_1 f_{\min} + C_2 f_{\min}^2$  and  $f = C'_0 + C'_1 P' + C'_2 P'^2$ ), the coefficients were calculated from the various data read from the backscatter ionograms using a regression method. Therefore the minimum group path and its derivative were obtained easily from the above equations so that the reflection virtual height can be derived from a general equation developed by *Jiao and Zhu* [1985]. The other calculations are carried out exactly as before. These

methods were developed based only on backscatter ionograms without requiring any other data, such as ionospheric parameters. Therefore it was frequently used in the OTHR experiments.

### 7.3. Relative Location Method

The relative location method was based on the principle of a circuit network and the quasi-parabolic electron concentration of ionosphere developed by *Croft and Hoogasian* [1968], where the ionosphere is considered to be an intermediate network [*Li and Jiao*, 1991]. A coherent transponder is introduced downrange and used as a reference point for the targets [*Huang and Li*, 1986]. With this method, it is necessary to set up a series of coherent reference transponders distributed appropriately, making it unnecessary to obtain real-time downrange ionospheric parameters. From the formulae given by *Croft and Hoogasian* [1968], for two transponders close to the unknown target, we can obtain four groups of equations in which the ground ranges are known and the group paths and corresponding frequencies can be determined from the backscatter ionograms. Therefore the unknown variables are the three ionospheric parameters and the two elevation angles for different radio rays. We can, in a similar fashion, obtain four additional equations where only three quantities, for example, the two elevation angles of rays propagating to the same target and the unknown ground range, are the variables for the unknown target if the targets are close to the transponders. Because the ionospheric parameters are assumed in this case, other quantities such as group path can be measured from the ionograms. Finally, an equation system with eight equations can be solved quickly with a supercomputer, although the equation system is nonlinear. So the unknown ground range and elevation angle of the ray to the unknown targets can be obtained. The entire calculation procedure may be automatically controlled by the computer network.

## 8. Estimation of OTHR Availability

Unstable phenomena often occur in the ionosphere. Their effects on making OTHR systems inefficient or unable to detect the targets effectively have been studied extensively [*Jiao*, 1986b]. Interruption of the propagation channel can be caused by the following unstable phenomena: sudden ionospheric dis-

Table 2. The Unstable Phenomena Occurrences

Phenomena	Effect	Time	Occurrence Solar Activity		
			High	Low	Full Cycle
Sudden ionospheric disturbance	break of the channel	daytime	0.5	...	0.2
$f_oF < 2.5$ MHz	coverage > 1300 km	before dawn	...	1.5	1.5
$f_oF > 10$ MHz	coverage < 3200 km	noon	30.0	3.4	7.5
$E_s$ screen	coverage < 2000 km	daytime	1.4	4.6	3.0
Aurora	limit detection	night	1.0	...	1.0*
Spread $F$	limit detection	night	0.3	3.0	1.3

\* Thirty percent in midlatitude region of western hemisphere.

turbances (SIDs), ionospheric storms, nuclear explosions, auroral absorption, and polar cap absorption (PCA). Limitation of the coverage area is created by following variable phenomena:  $f_oF$  (the critical frequency of  $F$  layer) and the screening by the  $E_s$  layer. Influences of variable phenomena on OTHR detection may be due to aurora, spread  $F$ , meteor trails, semiscreening of the  $E_s$  layer, and traveling ionospheric disturbances (TIDs). These unstable or variable phenomena occur randomly and have a serious influence on OTHR systems. Therefore it is necessary to estimate OTHR availability.

8.1. Minimum Unavailability of OTH Radar

According to statistical data from midlatitude ionospheric stations in China, the occurrence of unstable phenomena is given in Table 2. The minimum unavailability of HF OTH radar as a function of range is given in Table 3. It can be seen from Table 3 that the minimum unavailability of HF OTH radar depends only on the ionospheric propagation conditions. It is, in one sense, insurmountable.

8.2. Relationship Between Detecting Energy and Availability

The availability of OTH radar is defined as the ratio of time that the radar takes to reach a given value of signal-to-noise ratio (SNR) within an interval of operating time. This time is influenced by the solar cycle, which is approximately the lifetime of a radar system. Therefore the reliability results should be obtained on the basis of long-period statistics so that a reasonable estimate can be derived so as to take into account the long-period environmental effects. In the analysis [Jiao, 1988], expected ranges of sunspot numbers over a full 11-year cycle, all seasons and all times, have been examined. The statistically estimated results as a function of range are useful ways to determine the required detecting energy  $C$  for a typical HF OTH radar [Jiao, 1986a]. In this procedure, the minimum of the availability must, as mentioned, be considered.

As an application, the situation in China's midlatitude region was considered [Jiao, 1986a]. For simplicity, the data were chosen as follows: January,

Table 3. The Over-the-Horizon Radar Unavailability Minimums

phenomena	Distance, km			
	800-1300	1300-2000	2000-3200	3200-4000
Sudden ionospheric disturbance	0.2	0.2	0.2	0.2
Aurora	1.0	1.0	1.0	1.0
Spread $F$	1.3	1.3	1.3	1.3
$f_oF < 2.5$ MHz	1.5	...	...	...
$f_oF > 10$ MHz	...	...	...	7.5
$E_s$ screen	...	...	3.0	3.0
Total	4.0%	2.5%	5.5%	13.0%



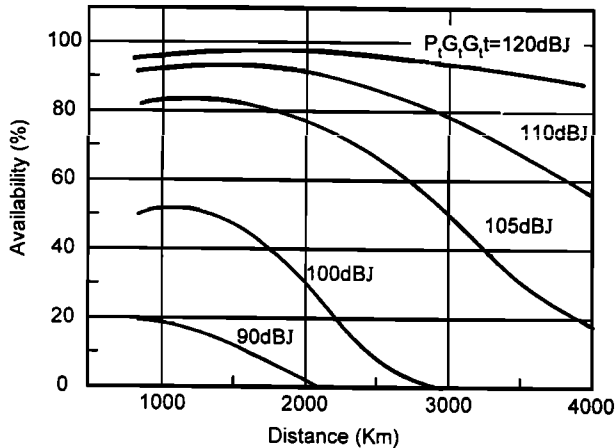


Figure 4. HF OTH radar availability at a given level of detectability.

April, and July; 0300, 0700, 1100, 1500, 1900, and 2300 UT (1100, 1500, 1900, 2300, 0300, and 0700 LT); and sunspot numbers 20, 70, and 120. Then, the relative wavelength, ionospheric loss, atmospheric radio noises for given distances  $D$  (in the 1000- to 4000-km range and 5000 km per group) were calculated at all these times. It should be pointed out that the values are statistical. Thus, for each calculated range, 54 measure of  $C$  were obtained. The time percentages were calculated for  $C$  values of the given detecting energies required and multiplied by the minimum unavailability for different coverages. The final results are shown in Figure 4, which indicates that a detection energy between 110 and 120 dBJ is re-

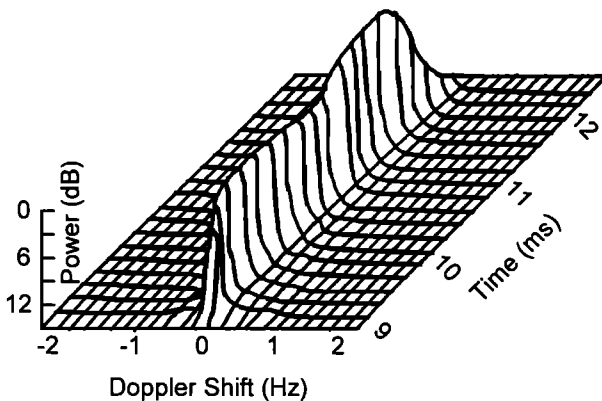


Figure 5. The spectra of the ground backscattered echoes as observed in a quiescent ionosphere.

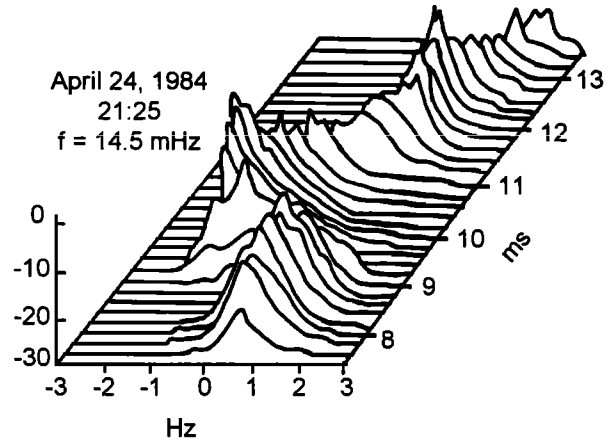


Figure 6. Spectra in the presence of traveling ionospheric disturbances as a function of frequency and time recorded on April 24, 1984, at a radar frequency of 14.5 MHz.

quired for good availability and that the most advantageous covered region is in the range between 1200 and 1300 km.

## 9. Extraction of Ionospheric Large-Scale TIDs Parameters

As an application of HF OTH radar, one has inverted the experimental data to obtain ionospheric parameters such as those of large-scale traveling ionospheric disturbances (LSTIDs) and irregularities. In this section, the inversion procedure used to determine ionospheric LSTIDs parameters from HF OTH radar will be introduced.

When the ionosphere was in a "quiet" state, ionograms showed very clear echo signatures and there was no distortion on the spectrum of pulse that propagated obliquely through the ionosphere and was scattered from the Earth's surface [Zhang *et al.*, 1988]. Representative ground-echo spectra are shown in Figure 5.

The experimental observations showed that either natural or artificial events cause ionospheric perturbations which were often observed. The following event is a typical LSTIDs: Figure 6 shows the three-dimensional Doppler spectra at 1325 UT (2125 LT) on April 24, 1984. It can be seen that there exist multiple peaks in the Gaussian-shaped spectra. It can also be seen that at different time delays there exist different Doppler frequencies, and as the time delay

changes the Doppler frequency changes from positive to negative, and vice versa. This represents the variation of the equivalent reflection surface as a function of time as it moves up and down. The corresponding maximum velocities are  $-55.7$ ,  $+48.5$ , and  $-24.3$  m/s, respectively. The following characteristic parameters of the LSTID were calculated using the fast Fourier transform: horizontal maximum main wavelength,  $\sim 2165$  km; horizontal propagation velocity,  $\sim 451$  m/s; azimuth movement direction,  $\sim 193.3^\circ$ ; vertical movement amplitude,  $\sim 93$  km, and average height of equivalent reflecting surface region, 320 km.

In addition to the previously discussed LSTIDs, many other TIDs have been observed. For example, the LSTIDs parameters observed at 0900–1200 UT (1700–2000 LT) on January 5, 1983, at an operating frequency of 14.5 MHz were the following: the horizontal movement velocity, 277.8 m/s; the horizontal wave length, 1346 km; and the vertical movement amplitude, 43.5 km. The parameters of an LSTID observed at 1300–1600 UT (2100–2400 LT) on April 25, 1984 were the following: horizontal propagation velocity, 386.7 m/s; horizontal maximum main wavelength, 1345.7 km; average height, 340 km; vertical movement amplitude, 38.3 km, and azimuth propagation direction,  $171.5^\circ$  (latitude).

## 10. Frequency Prediction Using Backscatter Ionograms

In general, frequency prediction is carried out using vertical ionospheric sounding data. In China, the oblique backscatter ionograms obtained from the OTH radar system have also been used for frequency prediction [Zhao, 1988]. In HF OTHR oblique sounding experiments, a large number of ionograms have been obtained. By using these ionograms to extract the ionospheric profiles, the diurnal variation of the critical frequencies was obtained. This approach was used to analyze propagation models for  $E$ ,  $E_s$ ,  $F$ , and mixed propagation modes, and to extract ionospheric propagation parameters, such as the optimum window of operating frequency, MOF, LOF,  $E_s$ MOF, etc.

Figure 7 shows the diurnal variations of observed frequency which were obtained from the 96 backscatter ionograms recorded by the OTHR systems on April 30, 1985. In the period of time between early night at 1300 UT (2100 LT) and the next morning at 2200 UT (06:00 LT), some strong interfer-

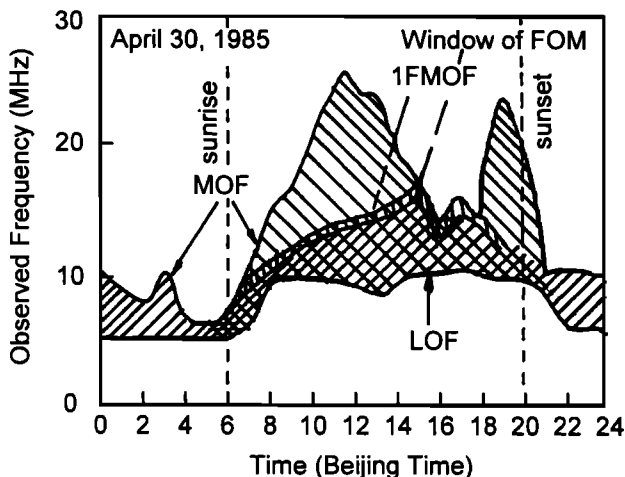


Figure 7. Diurnal frequency variations observed at a distance of 1500 km in April 1985.

ence occurred in HF communications. The frequency range chosen for communication is very narrow and is about 4 MHz. At 2100 UT (0500 LT), it is more difficult to communicate at this frequency, and only lower frequencies in the HF band could be used to maintain communication. The available frequency range shown in Figure 7 is only about 1 MHz. After 2200 UT (0600 LT), the communication conditions were much improved. The propagation models were expanded from  $E$  (or  $E_s$ ) layer model to the complex mode models. At about noon, the  $E$  (or  $E_s$ ) layer model was much more suitable for use in communications prediction.

Because the experiments were made in April and May, the probability of signal propagation in the  $E_s$  model becomes so high that the received signals are therefore very strong. Frequently, the maximum observed frequency of  $E_s$  layer ( $E_s$ MOF), is larger than  $F_2$ MOF. Therefore  $E_s$  can be used to transmit messages rapidly at a higher frequency when  $E_s$  is very strong because the time delay of the transmitted signal is very small relative to the normal case. Actual observation shows that the usable percentage of the  $E_s$  layer for HF communication is between 30 and 40% during April and May. An important result pertaining to the ionosphere in the east Asian region is that the probability of  $E_s$  is very high and the  $E_s$  is strong. However, when  $E_s$  becomes weak and  $F_2$  becomes stronger, the propagation mode in the  $F_2$  layer is then available for digital communication because at that time the transmitting rate is high.

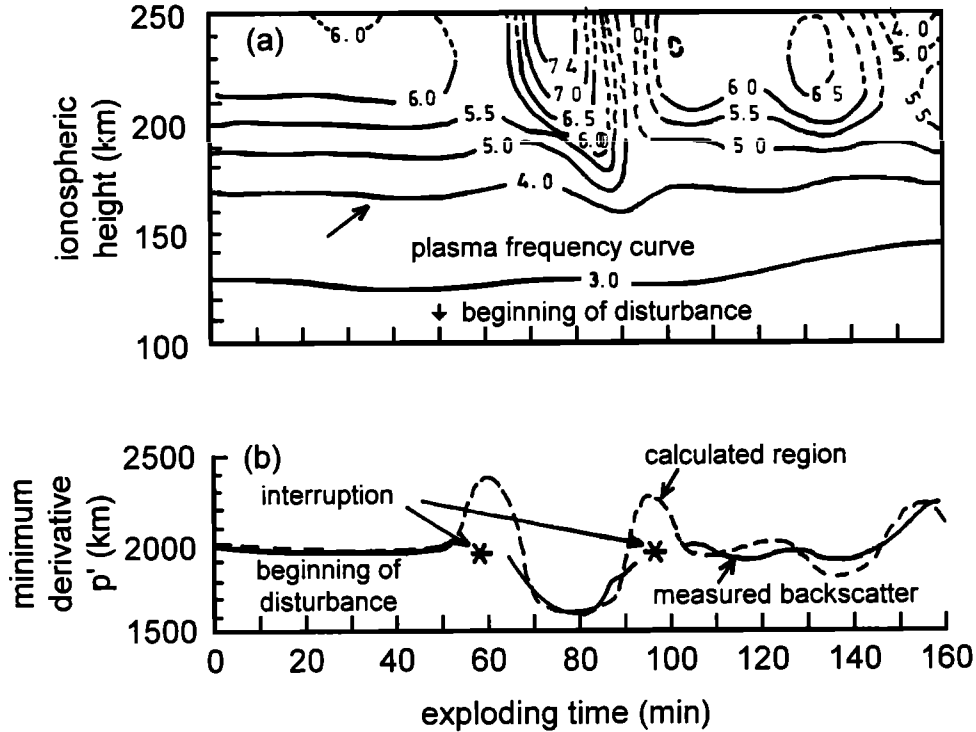


Figure 8. The effects of a nuclear explosion on OTH backscatter echoes. (a) Variation of plasma frequency as a function of time. (b) Temporal variation of the derivative of the observed minimum group delay.

### 11. Observation of a Remote Nuclear Explosion

In China, the experimental system of OTHR was used in 1976 to detect an actual nuclear explosion. In that observation, the HF OTH radar located at the Xinxiang radar base was 2205 km away from the nuclear explosion point. The operating frequency was 18.13 MHz, the power of the pulse waves was 10.8 kW, the antenna gain was approximately 32 dB, and the horizontal beamwidth used was 12°. A coherent transponder of 150 W was located to the east of the explosion site as a reference. Before the nuclear explosion, other instruments such as a vertical sounder and a high-frequency continuous wave Doppler measurement system were also set up, just below the nuclear explosion region to explore the variations of the upper ionosphere.

Figure 8 shows the plasma frequency in the reflection region (Figure 8a) and the derivative of the minimum group delay (Figure 8b) as a function of time. It can be seen from the contour diagram that the

constant plasma frequency is greatly perturbed. Figure 9 shows the ground spreading distance of the nuclear ionized region as a function of exploding time. The solid and dotted curves show the results observed from vertical and oblique backscatter soundings, respectively. In addition, Tables 4 and 5 show

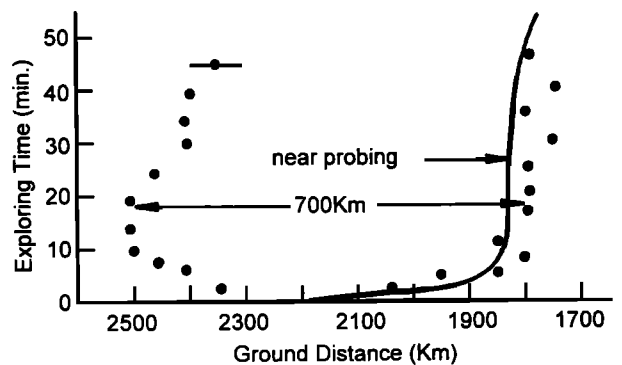


Figure 9. Temporal evolution of the ionized region near the time of the nuclear explosion.

Table 4. The Propagation Velocity of Disturbance in the Ionosphere

Observed Method	Name of Station	Distance of Explosion Point, km	Beginning Time of Disturbance, min	Propagating Velocity of Disturbance, m/s
Backscatter	Xinxiang	1400 (leading edge reflected region)	51	458
Vertical probing	Lasa	1260	43.4	484
	Lanzhou	1300	44.7	458
	Chongqing	1950	65.9	493
	Beijing	2200	74.5	492
	Wuchan	2450	85.1	480
	Guangzhou	2930	98.3	496

a comparison between the results obtained from various soundings. The results are in reasonable agreement with those obtained by other means, such as the vertical ionosonde set up below the explosion region.

## 12. Conclusion

In this paper, the high-frequency sky wave over-the-horizon backscatter radar systems in China, especially the Chinese phase I HF OTHR system, have been introduced, and the associated ionospheric backscatter studies in China have been briefly reviewed. The earliest Chinese HF OTHR (phase I) was a monostatic pulsed radar system supported by an ionosonde. It was built in the early 1970s primarily for scientific exploration of the environment, civil services, and military wide-area surveillance. The basic parameters and specifications of the Chinese experimental system are outlined in Table 1. In 1982, the first observations of aircraft were made, and from 1982 to 1984, several different types of civil aircraft were also successfully detected. With this OTHR system, two vertical carrier launchings of DF-2 and DF-5 rockets were observed in November 1989. To assist the Chinese OTHR operation, a real-time Chinese ionosonde network which serves as the world's largest ionosonde network has been set up jointly by the China Research Institute of Radiowave

Propagation and the Wuhan Institute of Mathematics and Physics. Since 1982, this experimental system has continued to serve in scientific and civil applications. Typical examples are (1) the extraction of ionospheric LSTID parameters, (2) frequency prediction using backscatter ionograms, and (3) observations of a nuclear explosion. In 1990s, the pulse Doppler system was changed to the current phase II frequency modulation (FM) continuous wave (CW) system, and the scanning beam direction was also changed. So the new phase II system is currently in operation and will continue to serve Chinese scientific, educational, and industrial institutions in the future. In addition to the OTH sky wave backscatter radar system (phases I and II), run jointly by the China Research Institute of Radiowave Propagation and the Nanjing Research Institute of Electronics Technology, two other OTH ground wave radar systems are currently operated by Wuhan University and Harbin University of Technology.

Only those relevant and relatively important publications and research reports are included in this brief review. There are many other results of case studies conducted on the HF radar's area of illumination [Huang, 1987a], the ionospheric coherent integration time using the phase detection integral method [Huang, 1987b], distinct propagation models [Huang, 1987c], the Chinese OTHR frequency management system, and the remote sensing of ocean

Table 5. Various Methods Used to Observe Other Ionized Regions

Method	Cosmic Noise Measurement	Vertical Sounding	High-Frequency Communication	Short-Range Backscatter	OTH Backscatter
Time, min (maximum	9 ionized region)	...	5	8	10
Maximum radius, km	350	>270	400	360	350

states around China. Studies of the last two aspects have been carried out for several years by two operating OTH ground wave radar systems. This paper does not attempt to cover all of the research results (from published papers and internal reports) on Chinese OTHR systems and their relevant ionospheric physics and wave propagation, due in part to their sensitive nature.

**Acknowledgments.** The authors whose papers are listed in the references of the present paper, especially Pei-Nan Jiao (China Research Institute of Radiowave Propagation (CRIRP), e-mail: pn-jiao@public.zz.ha.cn), who helped in confirming some of the technical contents, are acknowledged, as are useful discussions with John A. Bennett (Department of Electrical and Computer System Engineering, Monash University, Victoria, Australia) and Peter L. Dyson (Department of Physics, La Trobe University, Victoria, Australia). Thanks also go to the reviewers and especially to Tom Berkey (the guest editor of this special section) for their constructive suggestions. Finally, the assistance of Kristine Jensen of the Space Dynamics Laboratory is acknowledged; she contributed to the editing of the manuscript.

## References

- Ahearn, J.L., S.R. Curley, J.M. Headrick, and D.B. Triza, Tests of remote skywave measurement of ocean surface conditions, *Proc. IEEE*, 62(6), 681-687, 1974.
- Anderson, S.J., and M.L. Lees, High-resolution synoptic scale measurement of ionospheric motions with the Jindalee sky wave radar, *Radio Sci.*, 23(3), 265-272, 1988.
- Barrick, D.E., J.M. Headrick, R.M. Bogle, and D.D. Crombie, Sea backscatter at HF: Interpretation and utilization of the echo, *Radio Sci.*, 2(7), 673-680, 1967.
- Croft, T.A., Computation of HF ground backscatter amplitude, *Radio Sci.*, 2(7), 739-746, 1967.
- Croft, T.A., Sky-wave backscatter: A means for observing our environment at great distances, *Rev. Geophys.*, 10(1), 73-155, 1972.
- Croft, T.A. and H. Hoogasian, Exact ray calculations in a quasi-parabolic ionosphere with no magnetic field, *Radio Sci.*, 3(1), 69-74, 1968.
- Du, J.H., and P.N. Jiao, The localization technique for the experimental HF skywave radar, *IEE Conf. Publ.* 284, 259-263, 1988.
- Earl, G.F., and B.D. Ward, The frequency management system of the Jindalee over-the-horizon backscatter HF radar, *Radio Sci.*, 22(2), 275-291, 1987.
- Georges, T.M., Progress toward a practical skywave sea-state radar, *IEEE Trans. Antennas Propagat.*, AP-28(6), 751-761, 1980.
- Headrick, J.M., and M.L. Skolnik, Over-the-horizon radar in HF band, *Proc. IEEE*, 62(6), 664-680, 1974.
- Huang, D.Y., A study on the HF radar illuminated area (in Chinese), *Chin. J. Space Sci.*, 7(4), 298-305, 1987a.
- Huang, D.Y., Phase detection integral method for measurement of the ionospheric coherent accumulative time (in Chinese), *Chin. J. Space Sci.*, 7(3), 224-228, 1987b.
- Huang, D.Y., Distinguish of the propagation modes in the HF backscattering soundings (in Chinese), *Chin. J. Space Sci.*, 7(2), 139-145, 1987c.
- Huang, X.W., and Y.J. Li, Determining the ground distance of objects using the leading edge of backscattering ionograms (in Chinese), *Chin. J. Radio Sci.*, 1(2), 36-42, 1986.
- Jiao, P.N., The availability of the OTH radar, in *Proceedings of CIE 1986 International Conference on Radar*, pp. 21-25, CIE, Nanking, 1986a.
- Jiao, P.N., The study of the ionospheric effects of a nuclear explosion observed at large distance utilizing the HF backscatter technique (in Chinese), *Acta Geophys. Sin.*, 29(5), 425-431, 1986b.
- Jiao, P. N. and J. H. Du, The applied investigation of HF backscatter propagation, in *Proceedings of the 1998 International Symposium on Radio Propagation (ISRP '88)*, pp. 523-526, CRIRP, Beijing, 1988.
- Jiao, P.N., A new method of track processing for HF skywave radar (in Chinese), *Acta Geophys. Sin.*, 19(1), 1-6, 1991.
- Jiao, P.N., and J.H. Du, Calculation of the ground distance of the echoes of discrete scatterer in HF backscatter ionogram, in *Proceedings of the IEE Fifth International Conference on Antennas and Propagation (ICAP'87)*, pp. 259-263, IEE, London, 1987.
- Jiao, P.N., and J.C. Si, Exploring artificial ionospheric hole using skywave OTH radar (in Chinese), *J. Wuhan Univ., Nat. Sci. Ed.*, A Special Issue on Radiowave Propagation, 37-42, 1991.
- Jiao, P.N., and Q.G. Zhu, A new method on determining ground distance corresponding to minimum time delay in HF backscattering, in *Proceedings of the IEE Fourth International Conference on Antennas and Propagation (ICAP'85)*, pp. 555-558, IEE, London, 1985.
- Li, L.W., and P.N. Jiao, Determination of ionospheric parameters and ground distance of target using HF backscattering ionograms (in Chinese), *Acta Geophys. Sin.*, 34(1), 115-119, 1991.
- Lipa, B.J., D.E. Barrick, J.W. Maresca, and C.C. Teague, HF radar measurements of long ocean waves, *J. Geophys. Res.*, 85(5), 4089-4102, 1981.
- Ma, T.H., and P.N. Jiao, Ionospheric studies and sounding at the CRIRP, *IEEE Antennas Propagat. Mag.*, 38(6), 64-67, 1996.
- Maresca, J.W., and T.M. Georges, Measuring rms wave

- height and the scalar ocean wave spectrum with HF skywave radar, *J. Geophys. Res.*, *85*, 2759–2771, 1980.
- Rao, N.N., Inversion of sweep-frequency sky-wave backscatter leading edge for quasiparabolic ionospheric layer parameters, *Radio Sci.*, *9*(10), 845–847, 1974.
- Rao, N.N., Analysis of discrete oblique ionogram traces in sweep-frequency sky-wave high-resolution backscatter, *Radio Sci.*, *10*(2), 149–153, 1975.
- Wang, J., and C.G. Wu, HF sky-wave backscatter over-the-horizon radar, in *Proceedings of the CIE 1986 International Conference on Radar*, pp. 84–89, CIE, Nanking, 1986.
- Wieder, A.B., Some results of a sweep-frequency propagation experiment over an 1150-km east-west path, *J. Geophys. Res.*, *60*, 395–404, 1955.
- Zhao, D.L., The frequency prediction by oblique ionogram, *Chinese Journal of Space Science* (in Chinese), *8*(2), 145–149, 1988.
- Zhang, X.J., P.N. Jiao, and B.W. Jiang, LSTID measured by the technique of the HF backscattering sounder (in Chinese), *Chin. J. Space Sci.*, *8*(2), 138–144, 1988.

---

L.-W. Li, Communications and Microwave Division, Department of Electrical Engineering, National University of Singapore, 10 Kent Ridge Crescent, Singapore 119260. (e-mail: LWLi@nus.edu.sg)

(Received October 1, 1997; revised May 1, 1998; accepted May 12, 1998.)